Supporting Information

Canfield et al. 10.1073/pnas.1720529115

SI Materials and Methods

Sample Collection. All samples for geochemical analysis where obtained from fresh drill core, where drilling was conducted with fresh water as the drilling fluid to minimize contamination (see also ref. 1). As mentioned in the main text, Xiamaling unit 5 was intercepted in two cores. In one, the very top was cored, and this was used for high-resolution μXRF scanning as explored immediately below. In a second core, ∼45 m of Xiamaling Formation unit 5 was recovered, and this was used for the rest of our geochemical analyses.

High-Resolution XRF Core Scanning. One of our cores intercepted the top of the unit 5 IF equivalent to a depth of 356 m in our stratigraphy (Fig. 2). A 70-cm-long Fe-rich section of this IF was analyzed by using an ITRAX μXRF core scanner (COX Analytical Systems 2011). This nondestructive analysis provided X-radiographic and optical images at high resolution (see further details in ref. 2) (Fig. S2). Before analysis, one side of the split core was lightly polished, and its smooth surface was cleaned with alcohol. The XRF core scanner was used in combination with a 2.2-kW rhodium (Rh) tube operating at 30 kV and 50 mA. The measurements were acquired at 100-μm increments with an exposure time of 20 s, yielding 7,000 data points for the section. XRF raw data are expressed as element intensities in photon counts and require definition of the elements for semiquantitative evaluation (2). Within the XRF spectra, individual element peaks were extracted by using the Q-spec software from COX Analytical Systems, and the conversion of photon counts to concentrations was calibrated through certified reference materials (USGS SGR-1 and MAG-1) that reproduced Fe_2O_3 and MnO to within 2% and 12% uncertainty, respectively (2). Peak fitting was validated by multiple data points, with an average mean square error of <2.0%. Still, errors may arise in both the calibration (based on SGR-1) and peak discrimination, and the results are considered as semiquantitative. Still, the contents of Fe (wt%) and Mn (wt%) measured from μXRF (Fig. S2) are comparable to those in samples at 355–357 m determined with traditional sample preparation and XRF analysis (also described below and shown in Fig. 4).

Major Elements and Trace Metals. Fresh core samples were collected and crushed to powders with a diameter of <75 μm. Samples were analyzed for major elements with μXRF (PW2404; Philips Electronics) at the Key Laboratory of Petroleum Geochemistry (KLPG) in China as described (1, 3). The relative SD (RSD) was <1.0% for the elements reported.

Trace metal concentrations were determined with an inductively coupled plasma mass spectrometer (Finnigan MAT, Element I) following the procedures described in refs. 1 and 3. Trace metal concentrations were quantified by using calibration solutions containing the elements of interest (Mo and V), and the RSD of each trace metal was <1.5%. Accuracies were also tested with the shale standard (GBW 03014) that was measured along with the samples. The concentrations of the elements of interest (Mo and V) were within 10% of their reported values.

XRD Analysis. XRD analysis was performed at the University of Southern Denmark with a Rigaku MiniFlex X-ray diffractometer using a 600 W Cu-kα source. Data were acquired through measurements of 10° per min over a range from 10° to 70° and analyzed in the PDXL Software, using the Inorganic Crystal Structure Database. Examples of XRD spectra for a high Fe sample before and after acid treatment is shown in Fig. S3.

TOC Determination. Samples for TOC concentration were measured in two ways. For samples containing >10 wt% Fe, TOC was determined with a LECO CS-230HC carbon–sulfur analyzer. For this analysis, between 0.100 and 1.000 g of dry powders were precisely weighed and transferred into porcelain crucibles. After this, 0.5 mL of 1.5 M HCl was added to each sample and left on a hotplate to react for 2 h. Then, the samples were heated to a temperature <80 °C, while 1.5 M hydrochloric acid was added dropwise until the sample did not further react. After this, the crucibles were placed on the filter pump and then rinsed with distilled water to remove the acid solution. Then, the samples were placed in the metal crucible holder and then dried to constant weight in the oven at 70–80 °C. Finally, 1.000 g of iron flux and 1.000 g of wolfram flux were added to each sample, and TOC values were determined according to the operation method of the LECO CS-230HC carbon–sulfur analyzer. The RSDs of TOC values were <2.0%.

For samples with <10 wt% Fe, TOC was determined through our Rock Eval analysis as explained below. We found that when samples contained above ∼10 wt% Fe, decomposition of siderite interfered with the Rock Eval TOC determination (Fig. S6), prompting our use of the more traditional LECO combustion method for these samples as described just above.

Rock Eval. Rock pyrolysis was performed at the KLPG by using Rock-Eval (Version 6) under a nitrogen atmosphere. Pyrolysis was performed under programmed heating from 300 °C to 650 °C at a rate of 25 °C/min. The first released hydrocarbons comprised the so-called S1 peak (thermo-vaporized free hydrocarbons), The next hydrocarbons were released during thermal cracking, and these comprised the S2 peak. Both the S1 and S2 peaks were measured with a flame ionization detector. The S3 peak comprised the CO and CO_2 liberated during the thermal cracking of the kerogen, and these were measured with an infrared (IR) cell. A final oxidation step with oxygen at 800 °C yielded the residual carbon (RC), determined as CO_2 liberated and measured by IR detection. The data were recorded and interpreted with the complementary software ROCKINT. Pyrolysis and oxidation curves of CO_2 were used to calculate the amounts of pyrolyzed carbon (PC; from S1, S2, and S3 peaks) and RC (4). TOC (wt%) was the sum of PC and RC. The instrument was calibrated by using the standard material [GBW (E) 070038a] with RSDs of S2 values <5.0%. Measured TOC data with Rock Eval (Version 6) are shown in Fig. 5 and Table S1.

HI was calculated as S2(mg/g) × 100/TOC(wt%). As noted above (see also Fig. S6), we found that TOC concentrations from Rock Eval were inaccurate with total Fe concentration >10 wt%. Therefore, in calculating HI, we used Rock Eval TOC results for sediments with total Fe of <10 wt% and standard combustion after decarbonation with a LECO C-S analyzer (as explored above) for total Fe > 10 wt%.

Kerogen Extraction and Stable Isotope Analysis. Pure kerogen was extracted from several samples through HCl and HF treatment as fully described in ref. 3. The organic carbon isotopes ($\delta^{13}C_{kerogen}$) and nitrogen isotopes ($\delta^{15}N_{kerogen}$) were measured on the extracted kerogens by using a Flush EA 1112 HT O/H-N/C combined with a Delta V Advantage mass spectrometer (Thermo Scientific). The mass spectrometer was standardized with

NBS-18 ($\delta^{13}C = -5.014‰$) and Chinese standards GBW04405 ($\delta^{13}C = 0.57‰$) and GBW04407 ($\delta^{13}C = -22.4‰$) with a RSD of 0.2‰ based on replicate standard analysis. Carbon isotope values were reported relative to the Vienna Pee Dee Belemnite (VPDB). Values of kerogen $\delta^{15}N$ were determined during the same combustion as for the kerogen $\delta^{13}C$. The mass spectrometer was calibrated against reference standard IAEA-N-1 (with a $\delta^{15}N$ value of 0.538‰) and NBS-14 (with $\delta^{15}N$ value of 0.00‰), with $\delta^{15}N$ values reported relative to air. The SD of $\delta^{15}N$ was estimated at 0.2‰ based on replicate standard determination.

For the determination of carbonate $\delta^{13}C$ and $\delta^{18}O$, ~20 mg of rock powder were weighed and reacted with phosphoric acid in an online carbonate preparation device. This device was connected to a Finnigan Mat-252 mass spectrometer (Thermo Scientific), where the $\delta^{13}C$ and $\delta^{18}O$ were determined. The $\delta^{13}C$ and $\delta^{18}O$ were standardized with carbonate materials GBW04405 (with a $\delta^{13}C$ value of 0.57‰ and a $\delta^{18}O$ value of −8.49‰) and GBW04406 (with a $\delta^{13}C$value of −10.85‰ and a $\delta^{18}O$ value of −12.0‰), where $\delta^{13}C$ and $\delta^{18}O$ values were reported relative to VPDB, both with a SD of 0.2‰.

Biomarkers. Hydrocarbon extraction and biomarker analysis were performed at the KLPG. All analyses were performed on fresh drill-core material, drilled with fresh water as drilling fluid as described above. Our biomarker analysis was conducted as described (1, 3). However, in addition, we performed biomarker analysis both on the outside surfaces and inside sections of core material as described in ref. 5. Specifically, three samples with different contents of iron were collected and cut by using a Husqvarna TS350E core cutter and a ISOMET1000 precise cutting machine. Deionized water was used as lubricant to avoid contamination, and this was exchanged between samples. After cutting, both interior and exterior samples were crushed to powders and extracted.

Here, we focused on the alkylated trimethyl benzenes with fragment ion *m*/*z* 134 as the base peak. Among this fraction, we identified clear peaks for C13 to C23-2,3,6-TMAIs with the main peak of C18 and C19 as shown in Fig. S7. The reproducibility of the lower carbon number peaks was somewhat inconsistent in comparing inside and outside samples, and we took this to reflect volatility of these lower-molecular-weight compounds during sample extraction and measurement. In contrast, all inside and outside samples had nearly identical peaks for carbon numbers of C17 and higher, suggesting that these molecules were indigenous to the sample.

The 2,3,6-TMAIs were derived as the breakdown products of, ultimately, carotenoid pigments associated with brown strains of GSB (*Chlorobiaceae*) (6), themselves, anoxygenic phototrophic bacteria. Thus, the presence of 2,3,6-TMAIs indicated the presence of anoxygenic phototrophs in the ecosystem at the time of unit 5 deposition (see main text for further details). Although the concentrations we measured were low compared with other units in the Xiamaling Formation, they were much too high to arise from laboratory air exposure contamination during sample processing (7) as explored in ref. 1. These biomarkers were also absent from Jurassic sediments overlying the Xiamaling Formation (3), adding support to our conclusion that they were indigenous to unit 5 sediments.

1. Wang X, et al. (2017) Oxygen, climate and the chemical evolution of a 1400 million year old tropical marine setting. *Am J Sci* 317:860–899.
2. Croudace IW, Rindby A, Rothwell RG (2006) ITRAX: Description and evaluation of a new multi-function X-ray core scanner. *Geol Soc Lond Spec Publ* 267:51–63.
3. Zhang S, et al. (2017) The oxic degradation of sedimentary organic matter 1.4 Ga constrains atmospheric oxygen levels. *Biogeosciences* 14:2133–2149.
4. Lafargue E, Marquis F, Pillot D (1998) Rock-Eval 6 applications in hydrocarbon exploration, production, and soil contamination studies. *Rev Inst Fr Pet* 53:421–437.
5. French KL, et al. (2015) Reappraisal of hydrocarbon biomarkers in Archean rocks. *Proc Natl Acad Sci USA* 112:5915–5920.
6. Brocks JJ, Summons RE (2004) Sedimentary hydrocarbons, biomarkers for early life. *Treatise on Geochemistry, Biogeochemistry*, eds Holland HD, Turekian KK (Elsevier, Amsterdam), Vol 8, pp 64–115.
7. Illing CJ, Hallmann C, Miller KE, Summons RE, Strauss H (2014) Airborne hydrocarbon contamination from laboratory atmospheres. *Org Geochem* 76:26–38.

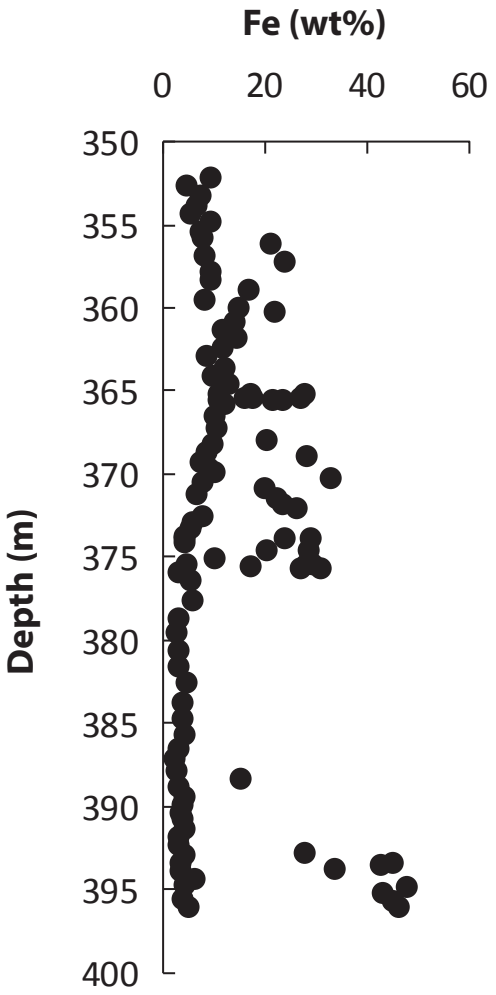

Fig. S1. Total Fe for the full depth of Xiamaling Formation unit 5.

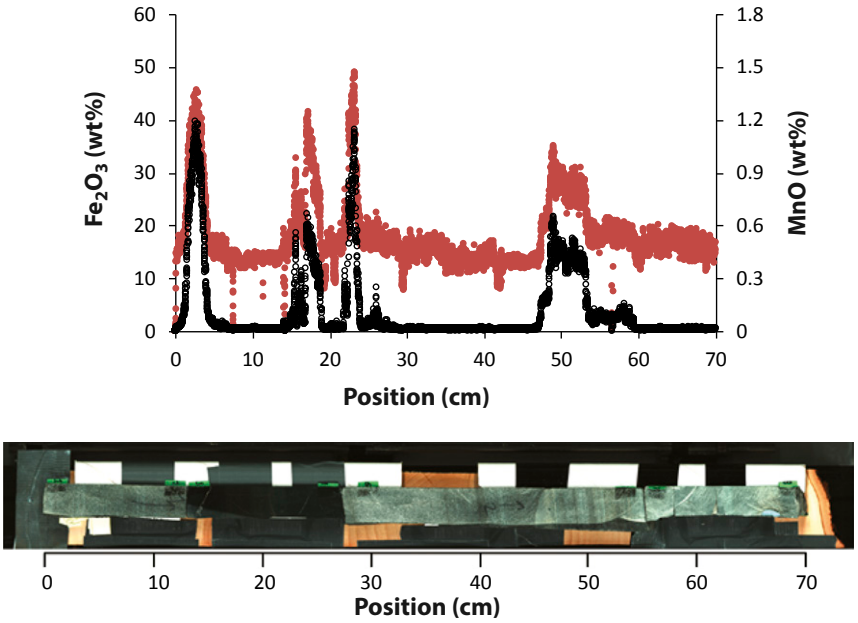

Fig. S2. μXRF results for the uppermost Fe-rich layer of Xiamaling Formation unit 5. Shown also is a photo of the scanned section, where the interval between 12 and 27 cm was polished to a higher degree and thereby is darker than the rest of the core section.

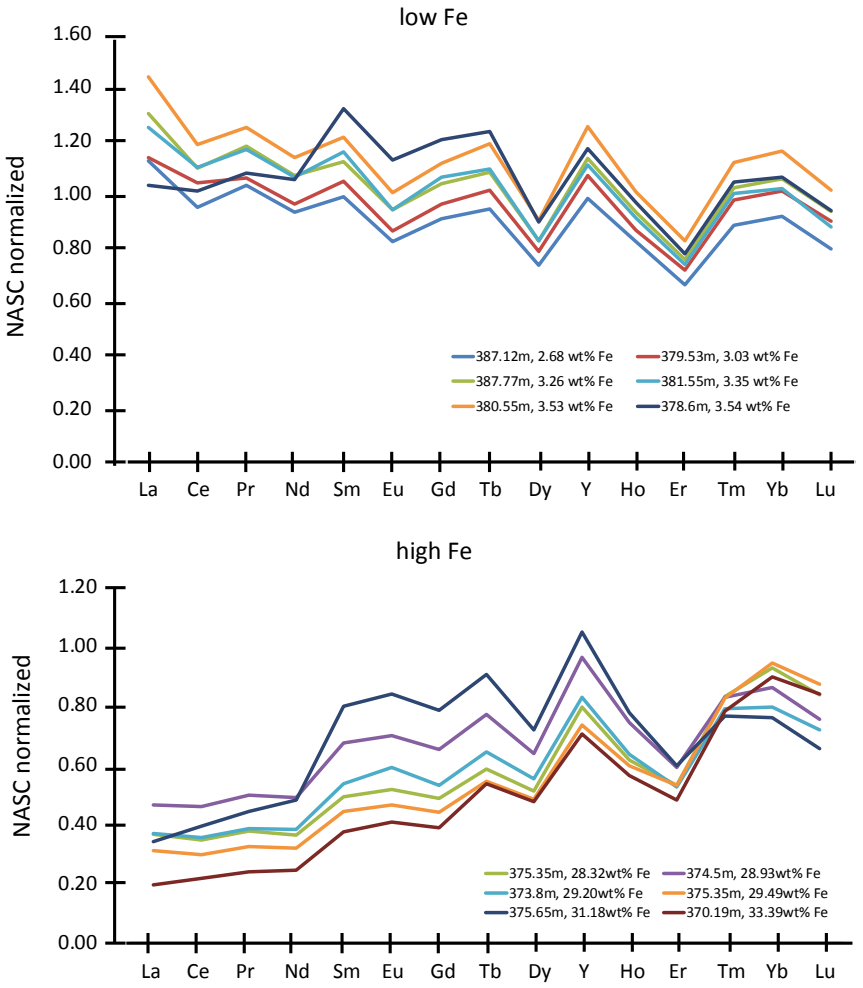

Fig. S3. Selected North American Shale Composite (NASC)-normalized REE plus yttrium patterns for low- and high-Fe samples from unit 5 of the Xiamling Formation. The complete set of data is in Table S2.

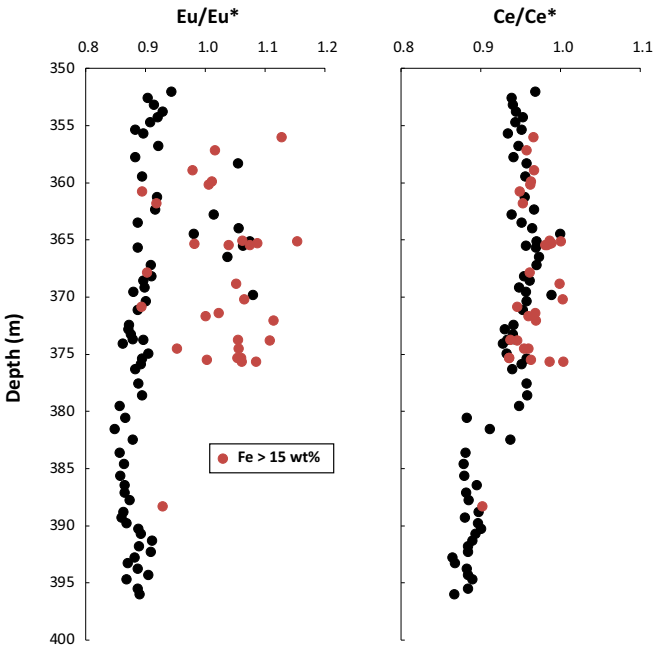

Fig. S4. Eu and Ce anomalies for unit 5 of the Xiamaling Formation. Samples with a total Fe content of >15 wt% are shown in red. The Eu anomaly (Eu/Eu*) was calculated from NASC-normalized values as Eu/0.5*(Sm+Gd), while the Ce anomaly was calculated as Ce/0.5(La+Pr) following ref. 1.

1. Bau M, Dulski P (1996) Distribution of yttrium and rare-earth elements in the Penge and Kuruman iron-formations, Transvaal Supergroup, South Africa. *Precambrian Res* 79:37–55.

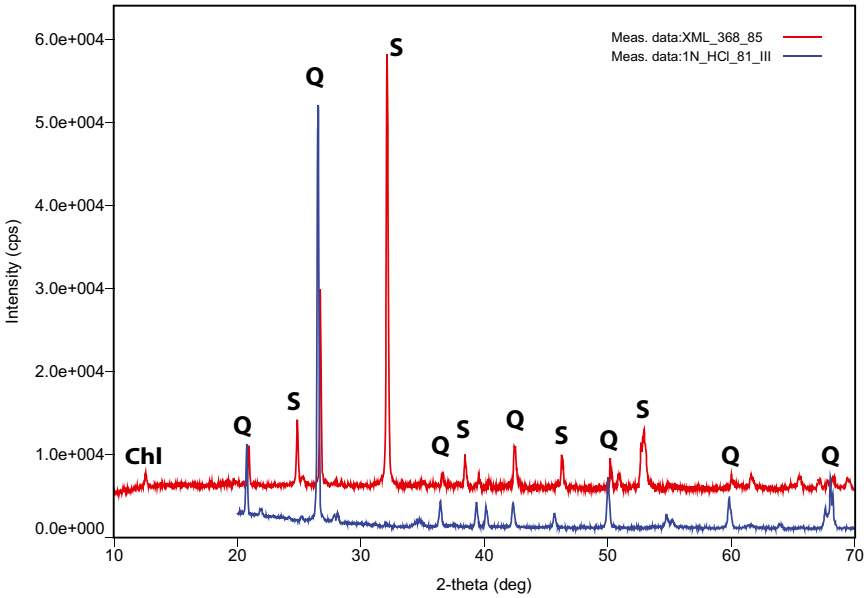

Fig. S5. XRD spectra of iron-rich interval from 368.86 m before and after acid treatment. Chl, chlorite; Q, quartz; S, siderite.

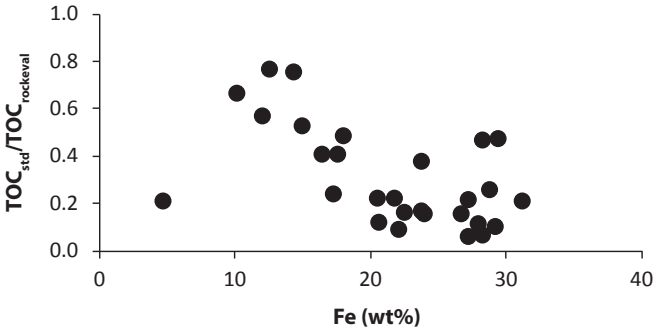

Fig. S6. Ratio of TOC measured by standard techniques (LECO; *Materials and Methods*) to TOC measured by Rock Eval vs. total Fe concentration.

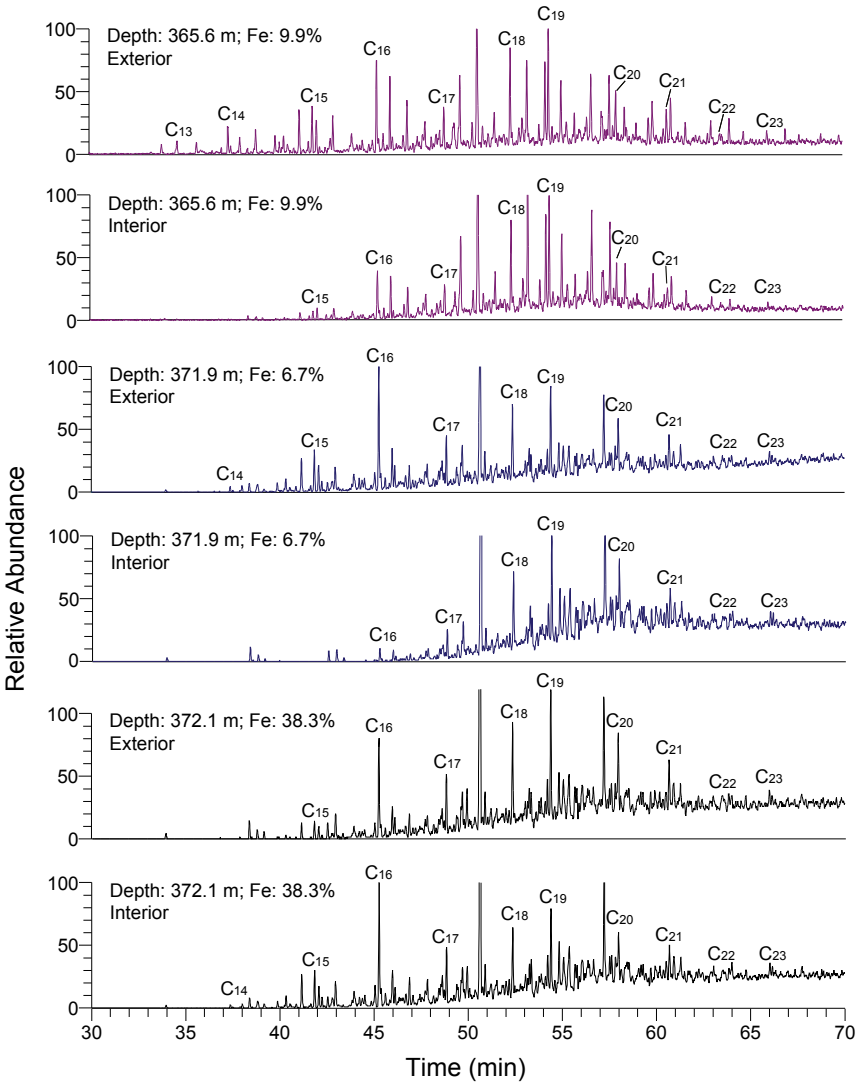

Fig. S7. GC-MS chromatograms (*m/z* 134) for the aromatic fraction of various depths in the Xiamaling Formation unit 5 for both inside and outside core sections.

Table S1. Geochemical data for unit 5 of the Xiamaling formation

Depth, m	TOC-whole rock, wt%	δ^{13}C-carb, per mil	δ^{18}O-carb, per mil	δ^{13}C-kerogen, per mil	δ^{15}N-kerogen, per mil	Tmax, °C	HI, mg/g TOC	OI, mg/g TOC	Al, wt%	Si, wt%	Fe, wt%	Mn, wt%	V, ppm	Mo, ppm
352.05	**0.04**						150	225	7.72	26.9	9.60	0.008	216	0.29
352.60	**0.21**			−32.1	6.32	453	90	52	8.50	29.5	4.90	0.009	203	0.46
353.20	**0.12**					462	83	67	7.20	29.0	7.80	0.013	219	0.32
353.80	**0.16**			−32.3	6.25	460	75	75	7.44	29.3	6.93	0.027	170	0.30
354.30	**0.19**					461	89	47	7.20	30.7	5.72	0.012	198	0.33
354.70	**0.21**			−32.5	6.87	454	81	48	7.10	27.5	9.85	0.012	165	0.37
355.35	**0.17**					454	94	65	7.26	29.4	7.66	0.010	199	0.28
355.70	**0.17**			−32.3	6.47	458	71	41	7.42	28.8	7.98	0.019	167	0.25
356.05						446		171	2.52	19.8	21.52	0.561	141	0.29
356.80	**0.17**			−31.9	6.32	454	100	53	6.73	29.5	8.62	0.009	183	0.28
357.15	0.10	−11.70	−4.40			444	21	221	3.13	16.8	24.00	0.909	102	0.23
357.80	**0.14**			−32.7	5.94	459	79	93	7.25	27.9	9.87	0.018	151	0.32
358.30	**0.63**					434	259	17	4.63	31.7	9.78	0.012	267	0.26
358.90	0.09	−19.50	−6.60	−33.4	6.05	492	22	225	3.98	23.2	17.26	0.236	118	0.19
359.45	**0.20**					465	80	50	6.42	30.4	8.36	0.009	182	0.24
359.90				−32.7	6.71	440	133	137	4.88	25.6	15.15	0.142	166	0.42
360.15	0.06	−21.00	−7.10			500	8	186	3.32	17.9	22.10	0.413	108	0.18
360.80	0.12			−31.1	6.83	462	50	244	6.21	25.4	14.39	0.094	124	0.53
361.25						475	56	206	6.46	27.1	12.19	0.065	153	0.23
361.80	0.14			−32.3	5.73	463	41	211	5.80	24.3	14.98	0.149	129	0.22
362.38	0.14					463	54	179	5.59	27.5	12.05	0.115	149	0.22
362.80	**0.08**			−32.4	5.49	448	88	275	3.69	34.1	9.05	0.010	175	0.34
363.50				−32.7	5.48	467	76	47	6.51	27.7	12.34	0.006	147	0.23
364.02						440	153	132	4.87	30.7	10.15	0.015	319	0.26
364.50				−33.1	6.49	503	91	109	5.82	28.0	13.41	0.008	182	0.22
365.10	0.10	−19.00	−8.10	−33.3	5.41	505	32	160	5.29	20.3	17.59	0.169	352	0.19
365.12	0.11	−27.00	−5.90			505	10	172	1.74	11.9	27.99	0.481	97	0.16
365.15				−32.9	5.72	439	124	153	4.32	31.4	11.39	0.019	221	0.29
365.31	0.22	−17.30	−7.30			445	11	179	1.96	12.6	27.20	0.501	97	0.16
365.35	0.19	−17.10	−7.90	−33.4	7.40	495	38	138	4.71	22.8	16.43	0.191	210	0.25
365.40	0.29	−20.60	−7.30			498	40	127	4.13	21.2	18.03	0.253		
365.45	0.14	−20.40	−6.20	−33.1	7.26	468	14	224	3.27	18.3	21.80	0.363	157	0.17
365.47	0.10	−20.90	−6.60			501	15	222	3.73	15.5	23.76	0.385	159	0.17
365.50				−32.9	7.46	444	89	137	4.96	29.7	11.11	0.038	275	0.23
365.70	0.14			−32.8	6.19	466	53	205	6.43	26.9	12.56	0.067	180	0.30
366.50						508	74	78	5.17	29.8	10.47	0.029	282	0.24
367.20				−33.1	4.84	460	95	55	6.55	28.3	11.01	0.008	211	0.28
367.85	0.09	−10.90	−4.90			460	17	261	4.94	20.1	20.51	0.320	115	0.81
368.18	0.13					455	55	170	7.11	27.5	10.15	0.071	198	0.28
368.60	**0.16**			−32.5	6.70	458	81	169	6.79	29.1	8.95	0.035	200	0.24
368.85	0.08	−10.30	−2.90			460	7	152	1.98	12.3	28.29	0.675	97	0.21
369.20	**0.14**					450	114	71	7.11	30.1	7.68	0.008	161	0.49
369.55	**0.19**			−32.6	7.29	470	74	21	6.86	28.4	9.34	0.007	190	0.25
369.85						470	85	100	4.97	30.8	10.43	0.008	209	0.27
370.19						460	5	137	1.13	7.9	33.29	0.718	58	0.15

Table S1. Cont.

Depth, m	TOC-whole rock, wt%	δ^{13}C-carb, per mil	δ^{18}O-carb, per mil	δ^{13}C-kerogen, per mil	δ^{15}N-kerogen, per mil	Tmax, °C	HI, mg/g TOC	OI, mg/g TOC	Al, wt%	Si, wt%	Fe, wt%	Mn, wt%	V, ppm	Mo, ppm
370.40	**0.14**			−33.0	6.70	455	112	47	7.07	29.5	8.23	0.011	194	0.26
370.85	0.22	−13.30	−5.70			458	20	122	4.78	19.2	20.40	0.340	112	0.23
371.15	**0.31**			−32.2	5.12	457	142	61	7.65	29.7	6.90	0.005	196	0.33
371.42	0.13	−14.80	−5.80			453	31	145	3.39	17.2	22.52	0.412	132	0.24
371.70	0.29	−8.10	−9.90			452	21	137	3.74	16.0	23.84	0.379	108	0.27
372.05	0.16	−11.20	−10.10			447	24	126	2.57	12.9	26.68	0.453	89	0.30
372.45	**0.14**			−32.4	6.24	449	129	64	7.12	30.0	8.09	0.007	162	0.36
372.85	**0.21**			−32.2		449	90	57	8.21	29.2	6.23	0.017	214	0.47
373.25	**0.14**					447	121	86	7.47	30.6	5.75	0.013	208	0.38
373.70	**0.26**			−31.8	5.98	443	185	96	8.69	29.6	4.78	0.007	187	0.46
373.75	0.18			−32.1	4.61	448	19	107	8.02	30.7	4.77	0.007	167	0.34
373.75						446	155	50	3.18	15.8	23.99	0.383	100	0.37
373.80	0.12	−13.50	−7.20			450	11	85	2.36	10.5	29.20	0.486	79	0.18
374.10	**0.21**			−32.4	4.20	442	110	43	8.32	30.2	4.47	0.014	204	0.35
374.50	0.15	−14.70	−5.00	−32.0	5.28	444	15	120	4.92	17.2	20.66	0.306	119	0.35
374.50	0.22	−14.30	−7.10			442	28	94	2.86	10.9	28.83	0.457	89	0.30
374.97				−32.2	5.50	444	91	50	7.62	26.9	10.56	0.006	145	0.20
375.35	0.57					446	7	159	2.63	10.6	29.49	0.816	77	1.40
375.35	0.55			−29.8		444	9	167	2.96	11.6	28.32	0.901	77	0.87
375.40	**0.15**			−31.9	4.71	442	107	87	7.19	31.3	4.97	0.023	195	0.68
375.50				−32.3	3.68	456	36	236	4.80	22.5	17.66	0.254	160	0.25
375.65	0.07	−14.70	−3.90	−32.2	3.84	440	11	152	2.51	13.1	27.25	0.438	61	0.41
375.65	0.28	−15.30	−3.90			446	11	128	2.16	9.3	31.18	0.507	84	0.26
375.90	**0.22**			−32.1	4.53	441	118	41	8.84	30.4	3.55	0.008	194	0.46
376.30	**0.19**			−32.1	4.17	442	111	26	8.94	29.0	5.87	0.006	161	0.49
377.56	**0.23**					442	135	39	8.90	28.6	6.02	0.009	191	0.69
378.60	**0.28**			−32.6	4.95	437	136	14	8.72	30.3	3.54	0.008	209	0.52
379.53	**0.24**					439	125	17	9.36	30.1	3.03	0.009	185	0.31
380.55	**0.34**			−32.2	5.07	437	118	9	9.69	29.3	3.53	0.007	167	0.51
381.55	**0.37**					439	119	14	9.22	30.4	3.35	0.003	167	0.59
382.50	**0.21**			−32.2	4.22	437	110	24	9.16	29.4	4.97	0.005	157	0.31
383.64	**0.34**					438	129	24	10.20	28.4	4.23	0.010	175	1.04
384.60	**0.32**			−32.4	5.60	437	94	25	10.14	28.7	4.39	0.005	161	0.38
385.65	**0.36**			−32.7		441	122	11	10.26	28.2	4.64	0.005	184	0.34
386.45	**0.35**			−32.0	5.83	440	151	9	9.44	30.2	3.54	0.004	144	0.42
387.12	**0.37**					440	124	14	10.04	30.0	2.68	0.005	164	0.55
387.77	**0.54**			−32.2	5.98	441	183	7	10.34	29.0	3.26	0.005	184	0.76
388.30						443		104	7.50	22.6	15.46	0.184	144	0.36
388.80	**0.66**			−32.3	6.30	440	208	8	10.31	29.2	3.58	0.005	198	0.79
389.30	**0.38**					441	108	13	10.06	28.4	4.76	0.007	185	1.19
389.80	**0.56**			−32.2	4.86	441	159	7	10.33	28.7	4.29	0.004	190	0.74

TOC data in boldface font are from Rock Eval.

Table S2. REE plus yttrium for unit 5 of the Xiamaling formation

Depth/m	Fe, wt%	La, μg/g	Ce, μg/g	Pr, μg/g	Nd, μg/g	Sm, μg/g	Eu, μg/g	Gd, μg/g	Tb, μg/g	Dy, μg/g	Y, μg/g	Ho, μg/g	Er, μg/g	Tm, μg/g	Yb, μg/g	Lu, μg/g
352.05	9.6	27.6	60.0	6.60	24.9	4.65	0.908	3.84	0.661	3.46	17.1	0.680	1.79	0.358	2.22	0.305
352.60	4.9	34.7	71.2	7.85	29.6	5.32	0.999	4.43	0.748	4.00	20.6	0.808	2.21	0.456	2.96	0.397
353.20	7.8	27.5	56.6	6.24	23.2	4.12	0.786	3.46	0.581	3.07	15.2	0.621	1.71	0.337	2.18	0.298
353.80	6.9	30.6	63.2	6.93	25.7	4.53	0.895	3.96	0.684	3.74	18.6	0.749	2.09	0.426	2.80	0.381
354.30	5.7	24.8	52.2	5.74	21.4	3.86	0.750	3.32	0.587	3.13	15.4	0.633	1.73	0.359	2.33	0.327
354.70	9.9	28.1	58.4	6.46	24.2	4.30	0.835	3.80	0.645	3.38	16.9	0.675	1.85	0.368	2.37	0.324
355.35	7.7	29.1	61.6	6.83	25.4	4.33	0.782	3.49	0.568	2.94	14.2	0.584	1.59	0.310	2.00	0.268
355.70	8.0	28.2	58.1	6.50	24.0	4.10	0.771	3.48	0.601	3.22	16.1	0.648	1.81	0.368	2.38	0.324
356.05	21.5	4.9	14.0	1.93	9.8	3.44	0.814	2.92	0.579	3.27	15.2	0.665	1.86	0.428	3.16	0.440
356.80	8.6	20.6	43.8	4.92	18.6	3.49	0.683	3.04	0.538	2.90	14.2	0.572	1.54	0.310	2.00	0.272
357.15	24.0	14.1	30.3	3.37	12.7	2.56	0.591	2.55	0.519	3.17	17.4	0.690	2.06	0.473	3.49	0.496
357.80	9.9	31.6	65.7	7.31	26.8	4.37	0.820	3.81	0.649	3.50	17.6	0.705	1.95	0.389	2.51	0.345
358.30	9.8	8.6	19.8	2.36	10.5	3.29	0.754	3.00	0.557	2.98	13.0	0.582	1.64	0.369	2.78	0.378
358.90	17.3	20.7	46.8	5.37	21.4	4.46	0.922	3.84	0.707	3.86	17.3	0.749	2.05	0.430	2.98	0.410
359.45	8.4	30.2	63.9	7.01	25.6	4.35	0.816	3.69	0.633	3.50	17.1	0.714	2.04	0.438	3.03	0.412
359.90	15.1	17.9	39.8	4.53	17.5	3.71	0.818	3.41	0.638	3.57	17.0	0.716	1.96	0.408	2.66	0.364
360.15	22.1	18.0	41.0	4.78	18.8	4.20	0.901	3.69	0.737	4.20	17.6	0.839	2.35	0.524	3.70	0.497
360.80	14.4	27.9	58.8	6.53	24.1	4.12	0.784	3.60	0.629	3.31	15.9	0.662	1.86	0.391	2.57	0.349
361.25	12.2	30.6	65.2	7.22	27.2	4.79	0.906	3.91	0.665	3.44	15.9	0.671	1.85	0.385	2.62	0.361
361.80	15.0	25.9	54.8	6.06	22.1	3.69	0.725	3.26	0.578	3.14	15.1	0.634	1.79	0.380	2.48	0.343
362.38	12.0	27.2	58.3	6.34	23.3	3.95	0.761	3.37	0.578	3.12	15.5	0.624	1.73	0.371	2.45	0.356
362.80	9.1	11.3	25.5	3.09	13.3	3.55	0.720	2.72	0.474	2.41	10.8	0.451	1.19	0.254	1.69	0.238
363.50	12.3	29.1	61.2	6.74	24.8	4.04	0.751	3.42	0.579	3.09	15.6	0.628	1.75	0.371	2.39	0.334
364.02	10.1	10.4	23.7	2.75	11.4	3.37	0.776	3.10	0.653	3.73	16.6	0.721	1.92	0.433	2.93	0.412
364.50	13.4	21.4	51.7	5.91	23.7	5.28	1.100	4.60	0.861	4.74	21.7	0.955	2.59	0.545	3.42	0.466
365.10	17.6	8.8	20.5	2.32	9.6	2.84	0.701	2.95	0.642	3.77	17.5	0.775	2.11	0.477	3.32	0.462
365.12	28.0	10.7	26.9	3.18	13.1	3.70	0.979	3.75	0.921	5.65	26.3	1.150	3.03	0.644	4.08	0.529
365.15	11.4	7.9	19.2	2.33	10.4	3.25	0.726	2.71	0.519	2.85	12.8	0.562	1.54	0.340	2.31	0.320
365.31	27.2	11.8	28.8	3.39	13.8	3.59	0.851	3.30	0.721	4.17	19.5	0.832	2.19	0.461	2.99	0.397
365.35	16.4	20.1	46.9	5.33	20.7	4.71	0.972	4.02	0.756	4.22	18.9	0.846	2.34	0.516	3.48	0.483
365.45	21.8	12.1	29.3	3.48	14.1	3.74	0.833	3.32	0.693	4.00	17.8	0.799	2.23	0.501	3.28	0.449
365.47	23.8	11.4	28.6	3.48	14.8	4.20	0.975	3.79	0.796	4.55	20.0	0.902	2.45	0.530	3.44	0.474
365.50	11.1	9.3	21.1	2.49	10.4	3.04	0.711	2.84	0.561	3.16	14.1	0.621	1.68	0.372	2.57	0.359
365.70	12.6	31.1	67.8	7.47	27.3	4.62	0.864	3.96	0.677	3.54	17.1	0.703	1.90	0.391	2.53	0.351
366.50	10.5	14.5	33.3	3.83	15.1	3.75	0.844	3.41	0.676	3.89	17.0	0.781	2.17	0.485	3.33	0.466
367.20	11.0	29.1	63.9	7.08	26.0	4.51	0.866	3.89	0.682	3.64	17.1	0.728	1.96	0.408	2.67	0.372
367.85	20.5	21.9	46.4	5.04	18.9	3.38	0.643	2.90	0.543	3.03	16.0	0.633	1.72	0.358	2.33	0.326
368.18	10.1	27.9	59.2	6.54	24.6	4.44	0.844	3.74	0.651	3.46	17.0	0.703	1.94	0.400	2.62	0.364
368.60	8.9	25.5	54.9	6.07	22.7	4.19	0.783	3.51	0.597	3.12	14.8	0.605	1.64	0.336	2.11	0.294
368.85	28.3	9.3	22.6	2.61	10.8	2.71	0.625	2.52	0.556	3.31	16.3	0.676	1.86	0.425	2.96	0.430
369.20	7.7	27.2	57.1	6.32	23.9	4.39	0.813	3.59	0.622	3.24	16.1	0.651	1.74	0.365	2.30	0.311
369.55	9.3	34.0	71.1	7.70	28.5	4.75	0.862	3.89	0.645	3.41	17.1	0.693	1.89	0.394	2.50	0.345
369.85	10.4	11.4	29.4	3.62	16.5	4.94	1.160	4.51	0.853	4.51	20.7	0.852	2.04	0.384	2.23	0.297
370.19	33.3	6.3	15.9	1.89	8.1	2.14	0.504	2.02	0.455	2.76	14.8	0.588	1.64	0.391	2.78	0.403
370.40	8.2	26.8	57.0	6.27	23.7	4.21	0.786	3.49	0.592	3.13	15.5	0.627	1.70	0.352	2.20	0.305
370.85	20.4	22.3	46.6	5.16	19.3	3.38	0.625	2.79	0.505	2.77	14.2	0.567	1.56	0.332	2.17	0.304

Table S2. Cont.

Depth/m	Fe, wt%	La, μg/g	Ce, μg/g	Pr, μg/g	Nd, μg/g	Sm, μg/g	Eu, μg/g	Gd, μg/g	Tb, μg/g	Dy, μg/g	Y, μg/g	Ho, μg/g	Er, μg/g	Tm, μg/g	Yb, μg/g	Lu, μg/g
371.15	6.9	34.7	73.4	8.11	31.0	5.35	0.968	4.28	0.713	3.72	18.3	0.738	2.03	0.424	2.67	0.364
371.42	22.5	8.6	20.2	2.39	9.7	2.38	0.520	2.10	0.421	2.30	10.9	0.454	1.20	0.260	1.65	0.229
371.70	23.8	15.1	32.7	3.65	14.2	2.92	0.613	2.48	0.489	2.77	14.4	0.570	1.55	0.337	2.19	0.304
372.05	26.7	10.5	25.4	3.08	13.4	3.68	0.897	3.40	0.684	3.80	20.0	0.768	1.98	0.431	2.77	0.389
372.45	8.1	34.6	70.7	7.72	28.8	5.05	0.918	4.23	0.719	3.81	20.4	0.790	2.14	0.456	2.82	0.379
372.85	6.2	36.1	73.7	8.24	31.1	5.39	0.961	4.34	0.713	3.72	18.9	0.741	1.99	0.410	2.52	0.351
373.25	5.7	30.2	62.8	7.00	26.2	4.76	0.863	3.93	0.659	3.45	17.6	0.689	1.88	0.387	2.41	0.330
373.70	4.8	39.4	81.2	8.93	33.4	5.73	1.020	4.52	0.743	3.84	19.4	0.766	2.09	0.425	2.60	0.358
373.75	4.8	33.9	69.6	7.77	29.3	5.07	0.936	4.14	0.693	3.65	18.5	0.734	1.98	0.400	2.50	0.336
373.75	24.0	12.1	26.1	3.04	12.3	2.79	0.630	2.47	0.483	2.76	14.7	0.567	1.53	0.330	2.11	0.295
373.80	29.2	11.8	26.0	3.04	12.6	3.06	0.734	2.77	0.546	3.20	17.4	0.660	1.79	0.394	2.46	0.345
374.10	4.5	37.6	76.7	8.62	32.0	5.61	0.996	4.59	0.758	3.98	20.5	0.810	2.21	0.454	2.76	0.379
374.50	20.7	23.8	51.4	5.72	22.2	4.62	0.916	3.86	0.718	3.92	20.4	0.804	2.17	0.432	2.82	0.384
374.50	28.8	14.9	33.6	3.94	16.2	3.84	0.868	3.40	0.654	3.70	20.2	0.772	2.01	0.414	2.67	0.362
374.97	10.6	34.3	69.9	7.76	29.0	5.60	1.070	4.82	0.830	4.33	21.7	0.831	2.21	0.427	2.65	0.353
375.35	29.5	11.7	25.4	2.99	12.0	2.80	0.643	2.54	0.497	2.97	16.7	0.641	1.81	0.415	2.87	0.401
375.35	28.3	10.0	21.7	2.56	10.5	2.53	0.577	2.29	0.463	2.81	15.4	0.622	1.81	0.413	2.92	0.418
375.40	5.0	25.8	54.9	6.04	23.0	4.49	0.826	3.66	0.625	3.27	16.1	0.668	1.77	0.357	2.31	0.318
375.50	17.7	14.3	31.9	3.64	14.4	3.14	0.679	2.82	0.529	2.89	14.2	0.582	1.55	0.317	2.10	0.285
375.65	27.2	10.7	26.4	3.15	13.7	3.56	0.845	3.29	0.642	3.62	20.4	0.729	1.91	0.378	2.32	0.309
375.65	31.2	10.9	28.7	3.50	15.9	4.54	1.040	4.09	0.769	4.16	22.0	0.807	2.03	0.382	2.35	0.314
375.90	3.6	35.5	74.7	8.24	31.7	6.19	1.150	5.18	0.865	4.47	22.2	0.901	2.44	0.483	3.14	0.429
376.30	5.9	39.9	81.7	8.98	33.1	5.97	1.110	5.11	0.877	4.54	23.1	0.919	2.44	0.500	3.19	0.428
377.56	6.0	34.8	73.5	8.02	30.7	5.82	1.090	5.00	0.891	4.71	23.9	0.955	2.57	0.521	3.37	0.456
378.60	3.5	33.1	74.0	8.54	34.8	7.53	1.400	6.28	1.050	5.21	24.6	1.010	2.65	0.523	3.30	0.451
379.53	3.0	36.4	76.1	8.39	31.8	5.99	1.070	5.02	0.864	4.56	22.5	0.902	2.44	0.489	3.14	0.432
380.55	3.5	46.1	86.7	9.88	37.5	6.92	1.250	5.81	1.010	5.23	26.3	1.050	2.81	0.560	3.60	0.488
381.55	3.4	40.0	80.5	9.24	35.1	6.61	1.170	5.55	0.930	4.80	23.3	0.950	2.51	0.502	3.17	0.422
382.50	5.0	38.4	79.8	8.96	34.0	6.36	1.150	5.19	0.877	4.52	21.8	0.876	2.32	0.462	2.90	0.390
383.64	4.2	47.4	89.1	10.20	38.5	6.72	1.190	5.53	0.944	4.87	24.5	0.978	2.66	0.534	3.36	0.454
384.60	4.4	48.4	91.5	10.60	39.6	7.08	1.260	5.78	0.981	4.99	24.8	0.990	2.60	0.516	3.28	0.444
385.65	4.6	48.2	91.0	10.50	39.2	6.98	1.240	5.77	0.977	4.94	24.7	0.996	2.62	0.522	3.27	0.434
386.45	3.5	33.0	64.3	7.41	27.9	5.14	0.939	4.42	0.747	3.88	18.9	0.769	2.03	0.396	2.51	0.341
387.12	2.7	36.0	69.5	8.18	30.8	5.65	1.020	4.74	0.805	4.27	20.7	0.856	2.25	0.443	2.85	0.382
387.77	3.3	41.7	80.2	9.33	35.3	6.39	1.170	5.42	0.921	4.79	23.8	0.971	2.57	0.513	3.28	0.449
388.30	15.5	27.9	56.3	6.63	26.0	5.32	1.050	4.64	0.859	4.76	23.9	0.967	2.62	0.520	3.37	0.469
388.80	3.6	41.0	80.4	9.27	35.5	6.63	1.170	5.34	0.897	4.59	23.1	0.910	2.44	0.478	3.07	0.431
389.30	4.8	45.7	86.5	10.00	37.7	6.72	1.200	5.59	0.954	5.00	25.2	1.010	2.69	0.522	3.35	0.463
389.80	4.3	39.3	77.0	8.89	33.3	6.04	1.080	4.93	0.848	4.36	21.9	0.876	2.37	0.466	2.92	0.402

Table S3. Biomarker data for the Xiamaling formation unit 5

Depth, m	TOC, %	TMAI- C18, μg/g TOC	TMAI-C19, μg/g TOC	TMAI- C18, ng/g rock	TMAI-C19, ng/g rock
353.80	0.16	0.07	0.07	0.11	0.11
354.70	0.21				
355.70	0.17	0.27	0.32	0.46	0.55
356.80	0.17				
357.80	0.14	0.10	0.10	0.15	0.14
358.90	0.40	0.16	0.16	0.65	0.63
359.90	0.43				
360.80	0.16	0.11	0.10	0.18	0.17
361.80	0.27	0.05	0.05	0.14	0.14
362.80	0.08				
363.50	0.17	0.09	0.12	0.15	0.20
364.50	0.11	0.25	0.28	0.27	0.31
365.10	0.25	0.18	0.26	0.45	0.66
365.15	0.17				
365.35	0.47	0.10	0.07	0.47	0.33
365.45	0.63	0.04	0.03	0.26	0.22
365.50	0.19	0.43	0.49	0.82	0.93
365.70	0.19	0.04	0.03	0.07	0.06
367.20	0.20	0.09	0.08	0.17	0.16
368.60	0.16	0.04	0.05	0.07	0.08
369.55	0.19	0.06	0.08	0.11	0.15
370.40	0.17	0.05	0.05	0.09	0.08
371.15	0.31	0.06	0.06	0.19	0.18
372.45	0.14	0.43	0.49	0.61	0.68
373.70	0.26	0.52	0.51	1.35	1.32
373.75	0.88	0.06	0.06	0.49	0.56
374.10	0.21	0.10	0.11	0.20	0.24
374.50	0.89	0.06	0.08	0.55	0.68
374.97	0.22	0.23	0.28	0.50	0.62
375.35	1.17	0.02	0.02	0.18	0.19
375.40	0.15	0.42	0.57	0.63	0.85
375.50	0.44	0.25	0.33	1.10	1.47
375.65	1.14	0.03	0.03	0.31	0.37
375.90	0.22	0.11	0.08	0.24	0.17
376.30	0.19	0.05	0.04	0.10	0.07
378.60	0.28	0.10	0.07	0.27	0.19
380.55	0.34	0.18	0.16	0.62	0.54
382.50	0.21	8.21	8.20	17.24	17.23
384.60	0.32	0.18	0.15	0.57	0.48
386.45	0.35	0.16	0.14	0.56	0.49
387.77	0.54	0.38	0.26	2.03	1.40
388.80	0.66	0.36	0.30	2.36	1.96
389.80	0.56	0.32	0.26	1.79	1.45
390.70	0.50	0.41	0.34	2.06	1.71
391.80	0.54	0.55	0.46	2.97	2.50
392.80	0.36	0.34	0.31	1.22	1.10
393.80	0.64	0.42	0.35	2.70	2.22
394.70	0.69	0.45	0.36	3.12	2.46
395.50	0.57	0.49	0.41	2.80	2.32